Korean J. Chem. Eng., **23**(4), 617-624 (2006)

Performance study on ultrafiltration of Kraft black liquor and membrane characterization using Spiegler-Kedem model

Projjwal Sarkar, Siddhartha Datta, Chiranjib Bhattacharjee†, Prashant Kumar Bhattacharya* and Bharat Bhushan Gupta**

Department of Chemical Engineering, Jadavpur University, Calcutta - 700 032, India
*Department of Chemical Engineering, Indian Institute of Technology (I.I.T.), Kanpur - 208 016, India
**IUT de Belfort-Montbéliard, Université de Franche-Comté, 90016 Belfort, France
(*Received 5 September 2005 • accepted 11 February 2006*)

Abstract–Ultrafiltration of Kraft black liquor was carried out by using an asymmetric membrane in a stirred batch cell, modified to work on a continuous mode. Spiegler-Kedem (SK) model from irreversible thermodynamics was used for the estimation of different membrane-solute parameters, like solute permeability (P_m) and reflection coefficient (σ). The P_m and σ so calculated from the above model were used to study the variation of these parameters with other process variables, like bulk concentration, pressure difference and stirrer speed. Finally, a simulation model was developed with the objective to predict permeate flux and rejection, which coupled the film theory, osmotic pressure model and SK model. The simulation results obtained from this study were validated with the experimental data using cellulose acetate membrane of 5,000 Da MWCO. Reasonably good agreements between the predicted and experimental values were observed and the average absolute deviation (AAD) for the prediction of flux and rejection using SK model was found to be 6.3%.

Key words: Ultrafiltration, Irreversible Thermodynamics, Film Theory, Parameter Estimation, Membrane Characterization

INTRODUCTION

In a conventional process the large amount of black liquor (BL) generated in pulp and paper industry is either discarded or treated in a destructive way to recover the inorganic chemicals at the cost of valuable organics. Ultrafiltration (UF) has already been suggested in different literatures [Olsen, 1980; Glimenius, 1980; Tsapiuk et al., 1989; Bhattacharjee and Bhattacharya, 1993] to recover these valuable organics, to meet a part of the water requirements and finally to tackle wastewater disposal problem due to strict environmental regulation. One of the major drawbacks in the use of UF for treating Kraft black liquor is the decline of flux with time. This may be attributed to gel formation, osmotic pressure retardation and fouling of the membrane resulting from reversible or irreversible pore plugging. Membrane fouling, which leads to decline of flux with time reduces the production rate and makes the process uneconomic in terms of time consumed since the system has to be stopped frequently to restore the flux by back flushing [Bhattacharjee, 2004]. Iritani and Mukai [1997] have investigated the flux and rejection in membrane filtration from physicochemical aspects. It was shown that the physical nature of the deposited cake-layer has an important effect on the filtration rate and rejection. A glass-ball inserted module design has been suggested by Kim and Kim [2003] to enhance the membrane flux. Effectiveness of this module was tested for three different modes of filtration: normal dead-end filtration, vortex flow filtration and enhanced vortex flow. It was found that for glass ball inserted membrane module the permeate flux tended to increase with increase in feed flow rate. A water treatment application of ultrafiltration process coupled with coagulation process has been reported by Jung and Kang [2003]. This work is based on detailed experimental investigation with an objective to remove natural organic matter (NOM). Thiruvenkatachari et al. [2005] have studied a new approach to a membrane hybrid system by pre-coating the hollow fiber membrane with powdered activated carbons (PAC) was evaluated for its ability to minimize the fouling of the membrane and to remove organic material from wastewater. Various other applications of ultrafiltration are being reported continuously in various journals.

The objective of the present work is to characterize the membrane by using the Spiegler-Kedem (SK) model. One of the specific features of this analysis is that the mass transfer coefficient could be obtained simultaneously with membrane parameters by nonlinear curve fitting. Much less amount of experimental data for parameter estimation is required for the proposed procedure. The variations of solute permeability and reflection coefficient obtained from the model have been studied with different operating variables and average values for both the parameters have been suggested, which are regarded as the properties of the membrane for the particular solute - membrane combination. Once the system has been characterized, a simulation model based on film theory and osmotic pressure model in conjunction with SK model has been suggested for the prediction of flux and rejection. Experimental data have been obtained from a stirred batch cell modified to work on continuous mode using cellulose acetate membrane of 5000 MWCO for model validation.

THEORY

Membrane transport models have so far been derived from two independent general approaches [Soltanieh and Gill, 1981]. The first one is the model based on non-equilibrium or irreversible ther-

†To whom correspondence should be addressed.
E-mail: cbhattacharyya@chemical.jdvu.ac.in

modynamics, where the membrane is treated as a black box in which comparatively slow processes are taking place near equilibrium. No information is required on the mechanism of transport for this approach. In the second approach, some mechanism of transport is assumed, and accordingly the fluxes are related to the forces that exist in the system. Thus, physicochemical properties of the membrane and system are involved in the model. In this study the Spieglar-Kadem (SK) model is used to estimate the different solute-membrane parameters. This model, based on irreversible thermodynamics, is combined with film theory to facilitate parameter estimation and then the simulation of flux and rejection under any specified operating conditions. The observed rejection (R_o), real rejection (R_r), volumetric flux (J_v) and mass transfer coefficient (k) can be correlated by the following expression which could be obtained from concentration polarization model [Bhattacharjee and Bhattacharya, 1993]:

$$\ln\left(\frac{1-R_o}{R_o}\right)=\ln\left(\frac{1-R_r}{R_r}\right)+\frac{J_v}{k} \tag{1}$$

Above equation will be used later to substitute for R_r in SK model.

1. Spiegler Kedem Model (SK)

This three-parameter model [Soltanieh and Gill, 1981] based on the concept of irreversible thermodynamics, starts with a differential equation for fluxes, given by

$$J_A=P_S\left(\frac{dC}{dx}\right)+(1-\sigma)CJ_v \tag{2}$$

Putting, $J_A=C_pJ_v$

$$P_S\left(\frac{dC}{dx}\right)+[(1-\sigma)C-C_p]J_v=0 \tag{3}$$

Integrating Eq. (3) with boundary limit as

$$x=0,\ C=C_p$$
$$\text{and } x=\Delta x,\ C=C_m \tag{3a}$$

$$\int_{C_p}^{C_m}\frac{dC}{(1-\sigma)C-C_p}+\int_0^{\Delta x}\frac{J_v dx}{P_s}=0 \tag{4}$$

which on integration gives

$$\frac{C_p-C_m(1-\sigma)}{\sigma C_p}=\exp\left[-\frac{J_v(1-\sigma)}{P_m}\right] \tag{5}$$

where $P_m=P_s/\Delta x$. Making R_r as the subject of equation

$$\frac{1}{1-R_r}=\frac{1}{1-\sigma}-\frac{\sigma}{1-\sigma}\exp\left[-\frac{J_v(1-\sigma)}{P_m}\right] \tag{6}$$

Substituting Eq. (1) in Eq. (6) to eliminate R_r will result,

$$\frac{R_o}{1-R_o}=\frac{\sigma}{1-\sigma}\left[1-\exp\left\{-\frac{J_v(1-\sigma)}{P_m}\right\}\right]\exp\left(\frac{-J_v}{k}\right) \tag{7}$$

In the above equation, the unknown parameters are as follows:

$$a_1=\frac{\sigma}{1-\sigma},\quad a_2=\frac{(1-\sigma)}{P_m},\quad a_3=\frac{1}{k} \tag{8}$$

2. Estimation of Parameter

The SK model is complex and non-linear. The two variables involved in this model are $[R_o/(1-R_o)]$ and J_v which are correlated by a nonlinear equation as given in Eq. (7). In this study experimental data were obtained at different sets of bulk concentration, stirrer speed and trans-membrane pressure (TMP), and the J_v & R_o were measured as a function of time under a fixed set of condition. Using the Larenberg-Marguardt [Press et al., 1992] non-linear regression technique, these data were curve fitted to get the values of the parameters a_1, a_2, a_3 under a fixed set of conditions, from which P_m, σ and k were calculated (using Eq. (8)). To estimate the final parameters, characterizing the membrane for the particular solute, the average values of P_m and σ obtained for all the experiments by this technique were calculated. These parameter values (i.e. P_m and σ) were used to simulate flux and rejection under particular operating conditions for the fixed solute - membrane combination.

3. Estimation of Diffusivity

The values of the mass transfer coefficient (k) for any stirred batch cell can be found from the well-known empirical correlation [Nguyen et al., 1980]:

$$k=0.0443\left(\frac{D}{r}\right)\left(\frac{\nu}{D}\right)^{0.33}\left(\frac{\omega r^2}{\nu}\right)^{0.8} \tag{9}$$

To predict diffusivity, Eq. (9) could be used after the k-values have been obtained under different operating conditions from the SK model. The viscosity and density of black liquor at different concentration were obtained from the correlation suggested in literature [Bhattacharjee and Bhattacharya, 1992; Finlayson, 1980]. The average of all the D-values obtained under different conditions has been taken as the desired value of diffusivity. The concentration dependence of diffusivity has not been considered in this analysis.

4. Simulation of Membrane Performance

The main objective in this work was to simulate volumetric flux and observed rejection (and hence permeate concentration) based on the membrane parameters (P_m and σ) determined by using the SK model. During the simulation, the mass transfer coefficient was determined by using the standard correlation, as given in Eq. (9) for the sake of generality, instead of using the curve-fitted values obtained through regression of Eq. (7). The predictions of volumetric flux and rejection were done by using Eq. (7) coupled with film theory and osmotic pressure model. Transient solution of convective-diffusion equation (resulting from film theory visualization of the mass transfer process) was done coupled with osmotic pressure model (Eq. (13)) to obtain the values of J_v & R_o (from C_p), and also C_m as a function of time.

4-1. Formulation of Convective-diffusion Equation

Under the condition of constant density & diffusivity the basic transport equation can be written as [Bhattacharjee and Bhattacharya, 1993]:

$$\frac{\partial C}{\partial t}=J_v\frac{\partial C}{\partial z}+D\frac{\partial^2 C}{\partial z^2} \tag{10}$$

The dependence of density on concentration has been allowed later. Under the following initial and limit conditions the above parabolic partial differential equation has to be solved:

$$\left.\begin{array}{lll} \text{i)} & \text{At } t=0, & C_A=C_b \quad \text{for all } z \\ \text{ii)} & \text{At } z=0, & C_A=C_m \quad \text{for } t>0 \\ \text{iii)} & \text{At } z=\delta, & C_A=C_b \quad \text{for } t>0 \end{array}\right\} \tag{10a}$$

Using orthogonal collocation (OC) technique Eq. (10) has now been expressed to reduce first and second derivatives in space coordinates to corresponding algebraic form to reduce it into a set of ordinary differential equations (ODE), corresponding to an initial value problem (IVP). Finally, the time derivative has been expressed in terms of an implicit formula, the Crank-Nicholson method [Finlayson, 1980]. Application of OC reduces the Eq. (10) to the following form for an $\underline{N}$ no. of internal grid point (written for i^{th} internal grid point):

$$\frac{dC_i}{dt} = J_v(t)\sum_{j=1}^{N+2} A_{ij}C_j + D\sum_{j=1}^{N+2} B_{ij}C_j = \Im_i(J_v(t), \underline{C}(t)) \quad (11)$$

where, $\underline{C}(t)$ represents concentration profile at time t, and could be expressed in the form of a vector as follows:

$$\underline{C}(t)=[C_1, C_2, \ldots, C_{N+2}], \text{ all at t.} \quad (11a)$$

Further, application of Crank-Nicholson method to estimate concentration at (k+1)-th time step gives:

$$\frac{C_i^{(k+1)} - C_i^{(k)}}{\Delta t} = \frac{[\Im_i(J_v^{(k+1)}, \underline{C}^{(k+1)}) + \Im_i(J_v^{(k)}, \underline{C}^{(k)})]}{2} \quad (12)$$

All the parameters (i.e., J_v, C_i for i=1…N+2) are known at k-th time step (say t_k) in the above equation, but are yet to be determined at (k+1)-th time step. Eq. (11); consequently, Eq. (12) can be written for all i, i=1, 2…N+1. Since the concentration remains constant at (N+2)-th grid point at all times (i.e., $C_{N+2}=C_b$ at all t), the corresponding equation has not been written. So, Eq. (12) represents (N+1) equations in (N+2) unknowns (C_1, C_2, …, C_{N+1} and J_v). Here C_1 is equivalent to C_m in earlier notations.

4-2. Osmotic Pressure Model

The volumetric flux may be determined as per the osmotic pressure model according to the following equation:

$$J_v(t) = \frac{\Delta P - \sigma\Delta\pi}{\mu_s R_m} \quad (13)$$

where, $\Delta\pi=\pi_m-\pi_p=\pi(C_m)-\pi(C_p)$

The osmotic pressure of a solution can be determined experimentally by using a membrane osmometer. The results from such studies were fitted by using the following polynomial equation. This is valid at least for the specific sample of BL used in this study [Bhattacharjee and Bhattacharya, 1992]:

$$\pi=42.9457C+0.1889C^2 \quad (14)$$

4-3. Simulation for Flux and Rejection

Using Eq. (12) and Eq. (13), coupled with SK model using corresponding membrane parameters, the permeate flux and rejection could be predicted without any experiment being performed at any desired operating condition, provided the corresponding membrane parameters are known. During the simulation it has been assumed that the membrane-solute parameters (P_m, σ) and membrane hydraulic resistance (R_m) are known *a priori* and accordingly, the proposed simulation model can be regarded as a three-parameter model.

The simulation is based on an iterative scheme, the algorithm of which is mentioned below:

(i) A specific value of Δt (time-scale increment) is selected.

(ii) Initialization step: At t=0, $C_m^{(0)}=C_1^{(0)}=C_b$, $C_p^{(0)}=0$ and $J_v^{(0)}=(\Delta P-\sigma\Delta\pi)/(\mu_s R_m)$ with $\Delta\pi=\pi_m-\pi_p$ (known for t=0)

(iii) Now Eqs. (7), (12) and (13) constitute a set of N+3 [N+1 number of equations from Eq. (12) and one each from Eqs. (7) and (13)]. The total number of unknowns at any instant of time corresponds to C_1 (=C_m), C_2, ..., C_{N+1}, C_p, J_v, i.e., a total set of N+3 unknowns. Multidimensional Newton-Raphson technique [Press et al., 1992; Finlayson, 1980] has been used to solve these N+3 equations with so many numbers of unknowns. For solution, an initial guess as specified in (ii) has been used for the first time step. A relaxation parameter has been used to enhance the convergence rate, which has been determined according to the Bryodens method [Press et al., 1992].

(iv) After convergence, a new set of values at $t_1=t+\Delta t$ have been obtained: $C_1^{(n)}$, $C_2^{(n)}$, …, $C_{N+1}^{(n)}$, $C_p^{(n)}$, $J_v^{(n)}$. Superscript 'n' corresponds to new value.

(v) $t=t+\Delta t$ and assignment of 'new' values to 'old' values, i.e., $C_1^{(0)} \leftarrow C_1^{(n)}$, $C_2^{(0)} \leftarrow C_2^{(n)}$ and so on.

(vi) Steps (iii) to (v) have been repeated up to the desired time to obtain a complete solution for concentration profiles, C_p & J_v as a function of time.

The value of Δt must be taken sufficiently small, otherwise there may be divergence even with relaxation parameter. In the present study, the Δt value was taken as 0.5 s in most of the cases.

MATERIALS AND METHODS

1. Materials

Concentrated black liquor (BL) was obtained from the Central Pulp Mills Ltd., Surat, Gujarat, India, based on Kraft process using mixed hardwoods, and its composition is reported in Table 1. Some other properties, related to characterization of wastewater are mentioned in Table 2, along with the corresponding quantities for UF treated BL. To get the desired concentration, BL was diluted with distilled water. Moist *spectra-por* type: C5 cellulose acetate (CA) complex membrane (asymmetric, molecular weight cut-off 5000 Da) was obtained from Spectrum Medical Industries® (USA). The membranes are usable in the pH-range 2-10; they are hydrophilic, resis-

Table 1. Composition of the raw black liquor

Total solids content	15.25%
Ash (or inert) content (dry basis)	28.13%
Sodium content	8.42 kg·m^{-3}
Water content	84.75%
Elemental analysis (dry basis)	
Carbon content	33.00%
Nitrogen content	nil
Hydrogen content	5.53%

Table 2. Estimation of parameters of raw and treated black liquor

Parameters	Raw black liquor	UF permeate black liquor
COD (ppm)	19000	980
BOD (ppm)	6300	350
Turbidity (NTU)	337	26.5
Conductivity (mMho/cm)	5.86	4.3

tant to temperatures up to 90 °C, and have low adsorption characteristics.

2. Apparatus

A stirred batch ultrafiltration cell was designed and fabricated with the following specifications:

Material of construction	: SS-316
Useful volume	: 450 mL
Residual volume	: nil
Filter diameter	: 76 mm
Effective filtration area	: 26.4 cm^2
Maximum testing pressure	: 3.5 MPa
Stirring facility	: mechanical, using a variable speed motor.

3. Analysis

Concentrations of BL were determined gravimetrically from samples dried at 150±2 °C. The viscosity and density were correlated to the concentration of BL at 30 °C as follows [Bhattacharjee and Bhattacharya, 1992]:

$$\mu_{BL}=(0.85+6.147\times10^{-2}C-1.117\times10^{-2}C^2+1.98\times10^{-3}C^3)/1000 \quad (15)$$

$$\rho_{BL}=(0.9953+0.4376\times10^{-2}C+0.398\times10^{-3}C^2)\times1000 \quad (16)$$

4. Design of Experiments

Experiments were designed so that the effects of three major independent variables, i.e., bulk concentration (20, 50 and 70 kg m^{-3}), pressure differential (550, 680 and 827 kPa) and stirrer speed (5.4, 7.5 and 8.8 rps) on flux and rejection can be properly measured. Two variables were held constant during the experimentation while the third was varied to get an exact picture of the dependences. All experimental runs were carried out at a fixed temperature of 30 °C with constant temperature bath.

5. Procedure

The membrane was placed on the porous support and the cell was assembled. The cell was pressurized with distilled water for at least two hours at 900 kPa (this pressure being higher than the highest level of pressure) to allow for initial compaction of the membrane. The constancy of the water flux beyond this time interval suggests no further compaction of the membrane. The membrane hydraulic resistance (R_m) was calculated from this constant water flux.

The stirrer speed (for the required rpm) was adjusted by regulating the voltage supply through a regulator after the cell was assembled with a cleaned and rinsed membrane. A proximity sensor was used to measure the rpm and it was connected to a digital display to facilitate smooth data recording. A constant voltage electric source was used to avoid any variation of rpm due to minor change in voltage. A metering pump was used to pump feed solution into the cell. Once the desired level of pressure was reached, the piston movement screw was adjusted to stop any further increase in pressure. An intermediate damper was also used to nullify the effect of any pressure fluctuation that may arise because of metering pump operation. The schematic diagram of the experimental setup is given in Fig. 1. The permeate was collected in a measuring cylinder and the volume was recorded as a function of time. The run was stopped when the permeate flow became steady, which was indicated by a nearly straight-line relationship between V and t. Once the V=f(t) has been obtained for any particular experiments, volumetric flux

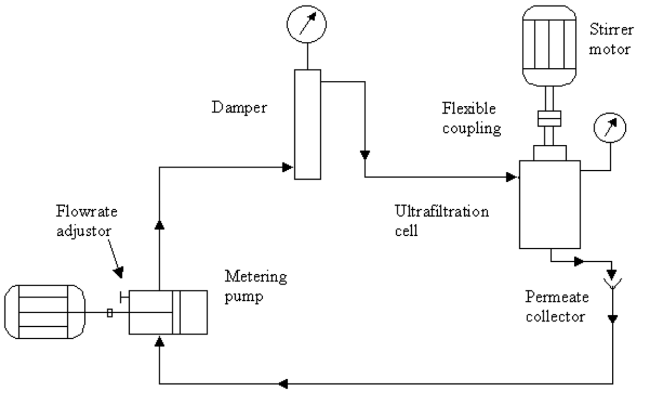

Fig. 1. Schematic diagram of the ultrafiltration set-up.

can be calculated using the relation:

$$J_v=\frac{1}{S}\frac{dV}{dt} \quad (17)$$

The permeate collected was intermittently recycled back into the cell by the same metering pump through an intermediate feed tank (not shown in the figure). During each experiment under fixed C_b, n and ΔP, data were recorded after every 15 min up to approximately 120 min for determination of flux and rejection at the specified time. Out of all the experimental data points, about 50% were used for parameter estimation and rests were used for model validation.

After each run, the membrane was thoroughly washed and rinsed with distilled water for at least two hours to remove any disposition. The water flux was then again checked to observe any variation in the membrane hydraulic resistance. The procedure was repeated for each set of operating conditions.

RESULTS AND DISCUSSIONS

Using the SK model the membrane parameters were first esti-

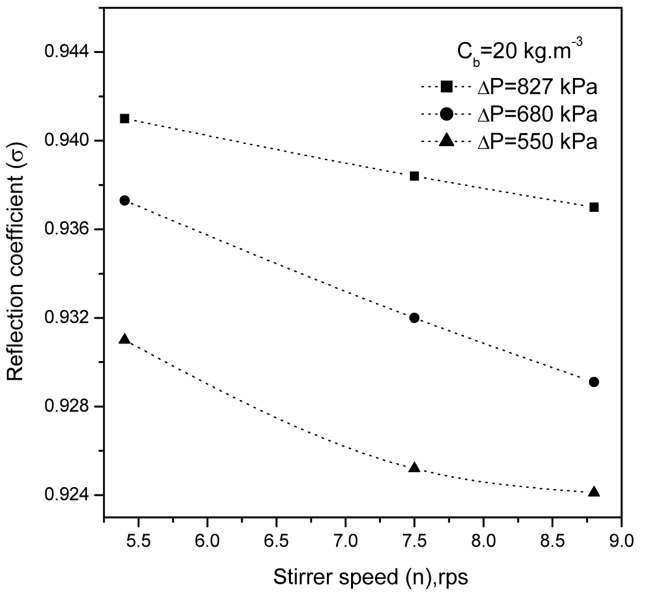

Fig. 2. Variation of reflection coefficient from SK model as a function of stirrer speed at different TMP at C_b=20 kg·m^{-3}.

mated following the procedure reported earlier and then these parameter values in conjunction with membrane hydraulic resistance (R_m) were used to simulate the flux and rejection at any specified operating conditions. Fig. 2 shows the variation of reflection coefficient with stirrer speed under different TMP, at fixed bulk concentration (C_b). It can be concluded that there is a decreasing trend for the reflection coefficient value with increasing stirrer speed. This behavior of reflection coefficient value with stirrer speed (n) and TMP can be explained by considering the fact that a reflection coefficient is a measure of the rejection capability of the membrane under a fixed set of operating conditions. Increase of reflection coefficient value with increase in TMP at fixed stirrer speed can be attributed to the higher rejection, resulting from the secondary membrane effect, which may come into the picture due to the deposition of the gel/polarized layer. Increased stirrer speed would cause higher turbulence near the vicinity of membrane, thus reducing the gel/polarized layer thickness and thereby reducing the secondary membrane effect, thus reducing rejection.

Variations of solute permeability (P_m) with stirrer speed under different TMP and at fixed bulk concentration have been shown in Fig. 3 which shows increased solute permeability at higher stirrer speed. Further, the solute permeability seems to decrease with increasing TMP. These observations could again be explained by using the concept of the deposition of the gel/polarized layer, acting as a secondary membrane layer, the thickness of which decreases with increase in stirrer speed, enhancing more solute permeability through the membrane. As the TMP increases, the deposited gel/polarized layer thickness increases due to more convective flow and higher rejection, causing the secondary membrane layer resistance to solute flow to increase. Due to this effect, the solute permeability is found to decrease with increase in TMP.

Fig. 4 shows the effect of change in bulk concentration and TMP on reflection coefficient at a fixed stirrer speed. This figure again confirms the observations made from Fig. 2, regarding the increase in reflection coefficient with increasing TMP. Further, the reflection coefficient was found to increase with increase in bulk concentration. This could again be explained by using the concept of secondary membrane. Higher bulk concentrations result more solute rejection near the membrane surface, causing the deposited gel/polarized layer thickness to increase, which may result in higher rejection and hence higher reflection coefficient. Variation of solute permeability with bulk concentration at different TMP under fixed stirrer speed has been shown in Fig. 5. This figure again shows the solute permeability value to decrease with increase in bulk concentration. Again, this may be explained with the same reasoning as stated earlier. Further, higher pressure causes the solute permeabil-

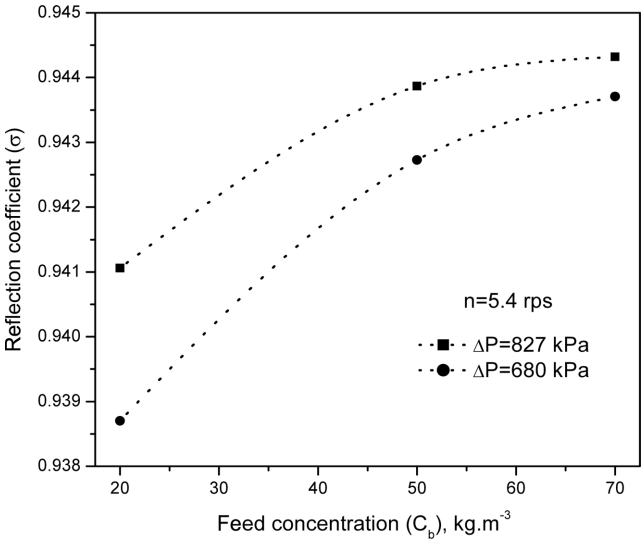

Fig. 4. Variation of reflection coefficient from SK model as a function of feed concentration at different TMP at n=5.4 rps.

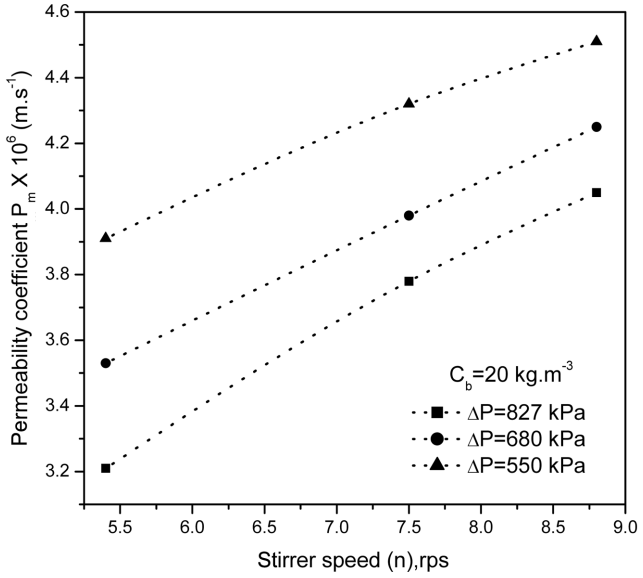

Fig. 3. Variation of solute permeability coefficient from SK model as a function of stirrer speed at different TMP at C_b=20 kg·m^{-3}.

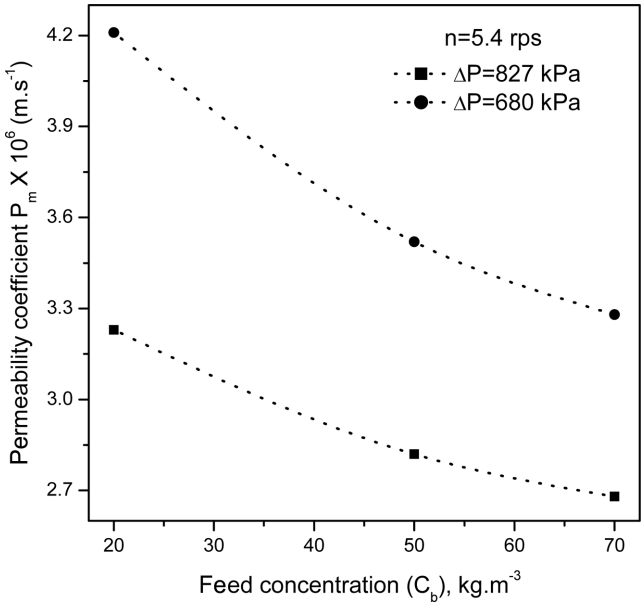

Fig. 5. Variation of solute permeability coefficient from SK model as a function of feed concentration at different TMP at n=5.4 rps.

ity to decrease because of the increased thickness of the deposited layer at higher TMP, as mentioned earlier.

During the simulation of flux and rejection, using the SK model, average values of σ and P_m have been used in the computation. The average values of reflection coefficient and solute permeability, so calculated, were 0.93663 (standard deviation=0.00599) and 3.685×10^{-6} m·s^{-1} (standard deviation=0.40402), respectively, from the SK model. The membrane hydraulic resistance, R_m was found to be 1.998×10^{13} m^{-1}. The proposed simulation approach is a three-parameter model, requiring the values of R_m, σ and P_m. Once, the above three-parameter values are known, calculations can be started to obtain the volumetric flux and permeate concentration as a function of time, starting from t=0 to any desired time. The initial guess values were observed to be very important for the solution of Eqs. (7), (12) and (13), constituting the set of (N+3) equations. The initialization step, as mentioned in step-2 of the proposed algorithm (given in §2.4.3), was found to provide convergence in all the circumstances. Further, the time increment (Δt) is an important user-defined parameter which has to be fixed *a priori*. Since an "A - stable" method has been used here for the solution of the initial value problem, as specified in Eq. (11), Δt was assumed to be 0.5 s, which was found to give reasonable accuracy with the proposed 2nd order implicit method.

Variations of permeate flux with time at different stirrer speed under fixed TMP and C_b have been shown in Fig. 6. The simulated permeate fluxes from the SK model have been compared with the corresponding experimental values. Permeate flux was found to increase with increase in stirrer speed which may be due to the reduced polarized layer thickness, resulting from the higher turbulence near the membrane surface. Experimental flux values at t=2h at different stirrer speeds are compared with predicted values from SK model; and have been shown in the inset of Fig. 6. For instance, the permeate flux prediction (at 120 min at 827 kPa TMP, 20 kg·m^{-3} bulk concentration and 8.8 rps stirrer speed) shows 3.39% deviation with SK model.

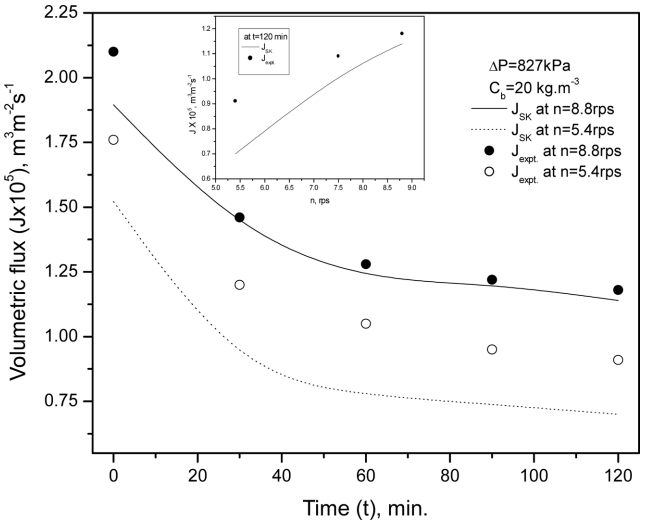

Fig. 6. Variation of permeate flux from SK model and from experiment as a function of time at different stirrer speed at C_b= 20 kg·m^{-3} and ΔP=827 KPa (inset). Variation of permeate flux from SK model and from experiment as a function of stirrer speed at t=120 min.

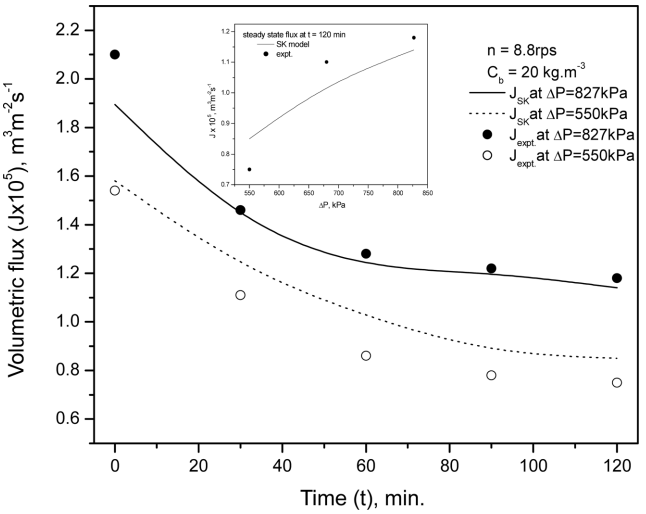

Fig. 7. Variation of permeate flux from SK model and from experiment as a function of time at different TMP at C_b=20 kg·m^{-3} and n=8.8 rps (inset). Variation of permeate flux from SK model and from experiment as a function of TMP at t=120 min.

Fig. 7 shows the variations of permeate flux with time at different TMP under fixed stirrer speed and bulk concentration. Both the experimental and predicted values of the flux show the declining tendency with time, characteristic of any pressure-driven membrane separation process. Permeate flux was found to increase with increase in operating pressure because of higher driving force; though, the increase gradually decreases at higher pressures (inset of Fig. 7), indicating the approach towards mass transfer controlled regime. Average absolute deviation (AAD) in the prediction of flux was found to be 6.3% for all the runs.

Variations of permeate concentration with TMP under different stirrer speed but at fixed bulk concentration have been shown in Fig. 8. Permeate concentration was observed to decrease with in-

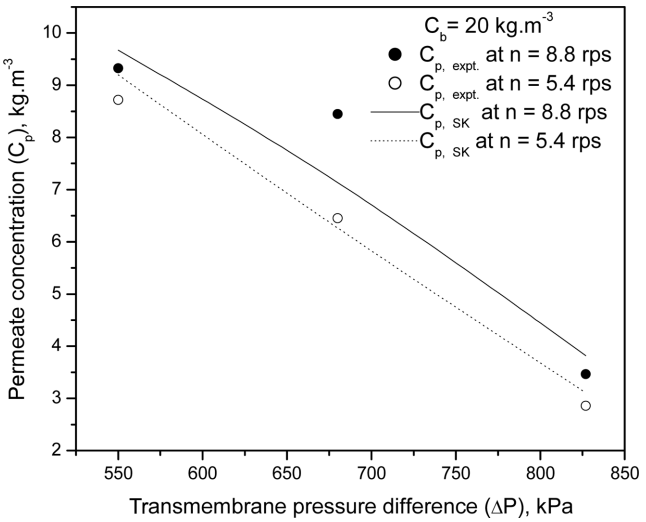

Fig. 8. Variation of permeate concentration from SK model and from experiment as a function of TMP at different stirrer speed at C_b=20 kg·m^{-3}.

crease in pressure. This implies higher rejection, which could be attributed due to the enhanced thickness of the deposited layer. Accordingly, this may cause more filtration of the solute by the so-called secondary membrane. Increases in stirrer speed cause increase in the permeate concentration, which can again be explained following the same logic as mentioned earlier. In most of the cases, the deviations in the prediction of flux and rejection were within ±10%. Accordingly, the proposed simulation algorithm seems to provide good results with regard to the prediction of flux and rejection.

CONCLUSIONS

A new method for membrane characterization has been proposed in this study, using thee SK model of irreversible thermodynamics. The reflection coefficient and solute permeability, so calculated, have been analyzed and the effects of change in the bulk concentration, stirrer speed and TMP on these parameters have been established. Detailed physical reasoning, explaining the variation of reflection coefficient and solute permeability with different operating variables, were discussed. Finally, a dynamic simulation model has been proposed which is capable of predicting permeate flux and rejection under any specified operating condition at any time. The proposed simulation model is a three-parameter model, comprising reflection coefficient, solute permeability and membrane hydraulic resistance. Simulation results were obtained by using solute permeability and reflection coefficient values, calculated by SK model. In fact, AAD for the prediction of flux and rejection using proposed simulation scheme was 6.3%. The predicted results from the model show good agreement with experimental data and are consistent with the assumptions inherent in the model and general notions regarding separation of macromolecular solutes by UF. Further, the proposed separation scheme is found to be very much effective in reducing COD and BOD by about 95% as shown in Table 2.

ACKNOWLEDGMENT

Some of the work in this study has been performed on equipment purchased under AICTE (TAPTEC) project (No. 8021/RID/NPROJ/TAP-6/2002-03), so the contribution of All India Council for Technical Education (AICTE), Govt. of India is gratefully acknowledged. Further, the authors acknowledge the funding received from the Indo-French Centre for Promotion of Advanced Research (IFCPAR) in partial support to this work.

NOMENCLATURE

AAD : average absolute deviation [-]
A_{ij} : element in the i-th row & j-th column position of the collocation matrix $\underline{A}$ [-]
a_1, a_2, a_3 : model parameters of the SK model, defined by Eq. (8) [-]
B_{ij} : element in the i-th row & j-th column position of the collocation matrix $\underline{B}$ [-]
BL : black liquor [-]
C : local solute concentration [$kg \cdot m^{-3}$]
C_A : solute concentration [$kg \cdot m^{-3}$]
C_b : feed concentration [$kg \cdot m^{-3}$]
C_m : membrane surface concentration [$kg \cdot m^{-3}$]
C_p : permeate concentration [$kg \cdot m^{-3}$]
D : diffusivity [$m^2 \cdot s^{-1}$]
J_A : solute flux through membrane [$kg \cdot m^{-2} \cdot s^{-1}$]
J_v : volumetric flux [$m^3 \cdot m^{-2} \cdot s^{-1}$]
k : mass transfer coefficient [$m \cdot s^{-1}$]
MWCO : molecular weight cut off [-]
n : speed of the stirrer [rps]
$\underline{N}$: number of internal grid points in orthogonal collocation method [-]
P_m : local solute permeability per unit membrane thickness [$m \cdot s^{-1}$] (permeability coefficient)
P_s : local solute permeability in the membrane [$m^2 \cdot s^{-1}$]
ΔP : transmembrane pressure difference [Pa]
R_m : membrane hydraulic resistance [m^{-1}]
R_o : observed rejection, $(1-C_p/C_b)$, (dimensionless)
R_r : real rejection, $(1-C_m/C_b)$, (dimensionless)
r : radius of membrane [m]
S : cross-sectional area of membrane [m^2]
SK : Spieglar-Kadem [-]
TMP : transmembrane pressure [-]
t : time [s]
UF : ultrafiltration [-]
V : volume of filtrate collected [m^3]
x : distance coordinate within the membrane with origin lying on the permeate side membrane surface [m]
Δx : membrane thickness [m]
z : distance away from the membrane surface on feed side [m]

Greek Letters

δ : film thickness [m]
μ_s : solution viscosity [$kg \cdot m^{-1} \cdot s^{-1}$]
σ : reflection coefficient, 0 for no rejection, 1 for total rejection
ω : stirrer speed [s^{-1}]
π : osmotic pressure [P_a]
Δ : difference [-]
μ : viscosity [$kg \cdot m^{-1} \cdot s^{-1}$]
ν : kinematic viscosity, (μ/ρ) [$m^2 \cdot s^{-1}$]
ρ : density [$kg \cdot m^{-3}$]
$\Im$: function, defined by Eq. (11)

Subscripts

b : bulk
i : component
m : membrane surface
p : permeate phase
j : component

REFERENCES

Bhattacharjee, C., "Analysis of continuous stirred ultrafiltration based on dimensional analysis approach," *Korean J. Chem. Eng.*, **21**, 556 (2004).

Bhattacharjee, C. and Bhattacharya, P. K., "Flux decline analysis in ultrafiltration of Kraft black liquor," *J. Membr. Sci.*, **82**, 1 (1993).

Bhattacharjee, C. and Bhattacharya, P. K., "Prediction of limiting flux

in ultrafiltration of Kraft black liquor," *J. Membr. Sci.*, **72**, 137 (1992).
Finlayson, B. A., *Nonlinear analysis in chemical engineering*, McGraw Hill, New York (1980).
Glimenius, R., "Membrane process for water, pulp and paper," *Desalination*, **35**, 259 (1980).
Iritani, E. and Mukai, Y., "Approach from physicochemical aspects in membrane filtration," *Korean J. Chem. Eng.*, **14**, 347 (1997).
Jung, C. W. and Kang, L. S., "Application of combined coagulation ultrafiltration membrane process for water treatment," *Korean J. Chem. Eng.*, **20**, 855 (2003).
Kim, J. P. and Kim, J. J., "Flux enhancement with glass ball inserted membrane module for the ultrafiltration of dextran solution," *Korean J. Chem. Eng.*, **20**, 99 (2003).
Nguyen, Q. T., Aptel, P. and Neel, J., "Characterization of ultrafiltration membranes, part-II. Mass transport measurements for low and high molecular weight synthetic polymers in water solutions," *J. Membr. Sci.*, **7**, 141 (1980).
Olsen, O., "Membrane technology in the pulp and paper industry," *Desalination*, **35**, 291 (1980).
Press, W. H., Teukolsky, S. A., Vetterling, W. T. and Flannery, B. P., *Numerical recipes in C*, Cambridge University Press, UK (1992).
Soltanieh, M. and Gill, W., "Review of reverse osmosis membranes and transport models," *Chem. Eng. Commun.*, **12**, 279 (1981).
Thiruvenkatachari, R., Shim, W. G., Lee, J. W. and Moon, H., "Powdered activated carbon coated hollow fiber membrane: Preliminary studies on its ability to limit membrane fouling and to remove organic materials," *Korean J. Chem. Eng.*, **22**, 250 (2005).
Tsapiuk, E. A., Bryk, M. T., Medvedev, M. I. and Kochkodan, V. M., "Fractionation and concentration of lignosulphonates by ultrafiltration," *J. Membr. Sci.*, **47**, 107 (1989).